
CONTROL ASPECTS FOR USING RIS IN LATENCY-CONSTRAINED MOBILE EDGE COMPUTING

A PREPRINT

Fabio Saggese[†], Victor Croisfelt[†], Francesca Costanzo[°], Junya Shiraishi[†], Radosław Kotaba[†],
Paolo Di Lorenzo[°], and Petar Popovski[†]

[†]Department of Electronic System, Aalborg University, Denmark

[°]Department of Information Engineering, University of Rome “La Sapienza”, Italy

[°]Consorzio Nazionale Interuniversitario per le Telecomunicazioni (CNIT), Parma, Italy
email: [†]{fasa, vcr, jush, rak, petarp}@es.aau.dk, [°]{francesca.costanzo, paolo.dilorenzo}@uniroma1.it

December 20, 2023

ABSTRACT

This paper investigates the role and the impact of control operations for dynamic mobile edge computing (MEC) empowered by Reconfigurable Intelligent Surfaces (RISs), in which multiple devices offload their computation tasks to an access point (AP) equipped with an edge server (ES), with the help of the RIS. While usually ignored, the control aspects related to channel estimation (CE), resource allocation (RA), and control signaling play a fundamental role in the user-perceived delay and energy consumption. In general, the higher the resources involved in the control operations, the higher their reliability; however, this introduces an overhead, which reduces the number of resources available for computation offloading, possibly increasing the overall latency experienced. Conversely, a lower control overhead translates to more resources available for computation offloading but impacts the CE accuracy and RA flexibility. This paper establishes a basic framework for integrating the impact of control operations in the performance evaluation of the RIS-aided MEC paradigm, clarifying their trade-offs through theoretical analysis and numerical simulations.

Keywords Reconfigurable Intelligent Surfaces, mobile edge computing, end-to-end latency, dynamic queue, control channels

1 Introduction

Beyond 5G networks are fundamental enablers of new services and applications (including verticals), such as Industry 4.0, Internet-of-Things (IoT), and autonomous driving [1, 2], which typically require massive data processing, high reliability, and low end-to-end delays. In this context, a key technical enabler is Mobile Edge Computing (MEC), whose aim is to allow proximity access to (albeit limited) cloud functionalities (*e.g.*, computing and storage resources) at the edge of the wireless network [3]. In MEC, user equipments (UEs) offload heavy computational tasks to nearby processing units or edge servers (ESs), typically placed close to access points (APs) of the radio access network, to improve energy consumption, reduce latency, and/or running sophisticated applications that would be impossible to execute at the UE side. However, the available network resources must be jointly optimized and orchestrated to provide the end users with a satisfactory quality of service (QoS). This problem has sparked a lot of interest in recent literature, with several works that have proposed joint resource optimization frameworks in both static and dynamic MEC scenarios, *e.g.*, [3–7].

In MEC systems, good wireless connectivity is a necessary condition for ensuring the required QoS. In the presence of poor wireless channel conditions, the performance of MEC systems might be severely hindered because of lower offloading rates and consequent under-exploitation of the computation capabilities of the ES. A substantial performance boost can be achieved by exploiting reconfigurable intelligent surfaces (RISs), an emerging technology that

*This work was partly supported by the Villum Investigator grant “WATER” from the Villum Foundation, Denmark, and by the EU H2020 RISE-6G project under grant number 101017011. (Corresponding author: Fabio Saggese, email: fasa@es.aau.dk)

has gained significant attention in recent years due to its ability to shape and control the wireless communication environment [8]. To this aim, several works have already investigated the optimization of RIS-aided MEC systems, considering both static and dynamic computation offloading [9–13]. These methods aim to jointly optimize the RIS configuration, the AP and UEs communication parameters, and the ES central processing unit (CPU) resources to provide a target QoS. In [10], the authors focus on maximizing the number of processed bits for computation offloading. Furthermore, [11] explores the utilization of RISs to enhance the performance of machine learning tasks at the ES. [12] suggests optimization-based and data-driven solutions for RIS-aided multi-user MEC, aiming to maximize the total completed task-input bits of all UEs within limited energy budgets. Lastly, [13] delves into the dynamic optimization of a RIS-empowered dynamic MEC scenario in which the UEs continuously generate data for offloading while wireless channel conditions evolve through time. The optimization aims to ensure minimum energy consumption under an average latency constraint.

To the best of our knowledge, the control operations needed for using RISs in MEC systems and their impact on the QoS experienced by the end user has never been investigated within the existing literature. The analysis of those procedures is central to enabling RIS-aided MEC services in future wireless networks. Among the first works on the subject is [14], which proposes a general method to include the control aspects in the performance evaluation of RIS-aided networks. By using similar considerations, this work defines and quantifies the impact of control operations on the performance of RIS-empowered MEC systems by focusing on the trade-offs and interactions between the amount of resources invested in the control procedures *vs* data transmission and computation offloading at the MEC. The analysis uses the MEC offloading strategy proposed by [13]. Our results show that control errors may disrupt the MEC service if not properly considered during the system design. While the results underline the necessity for high reliability of the control signaling, it is seen that the channel estimation (CE) procedure strongly degrades the performance. On one side, its high overhead reduces the end users' QoS, limiting the time reserved for offloading operations; on the other, errors in channel state information (CSI) estimation strongly affect the resource allocation (RA), and thus the optimality of the allocated resources.

Notation Boldface lower, \mathbf{x} , and capital, \mathbf{X} , letters denote vector and matrices, respectively; $\mathbf{0}_n$ is an n -size zero vector; \mathbf{I}_n is the $n \times n$ identity matrix; $\|\cdot\|$ is the Euclidean norm; \circ is the element-wise multiplication. Calligraphic letters, \mathcal{A} , denote sets; $|\cdot|$ denotes the absolute value if applied to a scalar or the cardinality if applied to a set. $\mathcal{CN}(\boldsymbol{\mu}, \boldsymbol{\Sigma})$ is the complex Gaussian distribution with mean value $\boldsymbol{\mu}$ and covariance matrix $\boldsymbol{\Sigma}$; $\mathbb{E}_{\sim x}[\cdot]$ is the expected value w.r.t. x .

2 System Model

We consider the RIS-aided MEC system depicted in Figure 1, where K single-antenna UEs want to offload computational-heavy tasks to an ES endowed with an M -antenna AP and aided by an RIS equipped with N -elements. For simplicity of notation, we collect the sets of UEs and AP antennas in $\mathcal{K} = \{1, \dots, K\}$ and $\mathcal{M} = \{1, \dots, M\}$, respectively. We assume that the UEs are multiplexed according to a frequency division multiplexing (FDM) technique, enabling them to transmit or receive simultaneously without interfering with each other [13]. Then, we let B be the total bandwidth allocated for communication between the AP and the UEs. We denote as B_k the bandwidth allocated to the k -th UE, such that $B = \sum_{k \in \mathcal{K}} B_k$.

Similar to [13], we consider that the offloading is dynamic; that is, the UEs continuously generate data that need to be processed by the ES. Hence, the system ends when the offloaded data of all UEs are entirely processed by the ES. In such a dynamic system, time is organized into *slots* of equal duration $\tau \in \mathbb{R}_+$, indexed by $t \in \{1, 2, \dots\}$. A slot is then further divided into control and payload parts as

$$\tau = \tau_{\text{ctl}} + \tau_{\text{pay}}. \quad (1)$$

Within the control time or *control overhead* τ_{ctl} , *control operations* are performed, which include: a) the CE used to obtain the CSI at the AP, b) the RA carried out by the ES and used to optimize the transmission parameters for the UEs, the processing parameters at the ES, and the RIS properties, and c) the control signaling used to exchange relevant information among all the nodes involved. The payload time τ_{pay} comprises the actual transmission/offloading of data by the UEs.

We aim to *minimize the total energy consumption of the system while keeping the offloading latency perceived by the UEs under a threshold*. In Section 3, we give detailed information on the protocol that dictates how the offloading service occurs on a slot basis when achieving this goal and considering the control operations. Below, we introduce the notation and models required to describe the protocol.

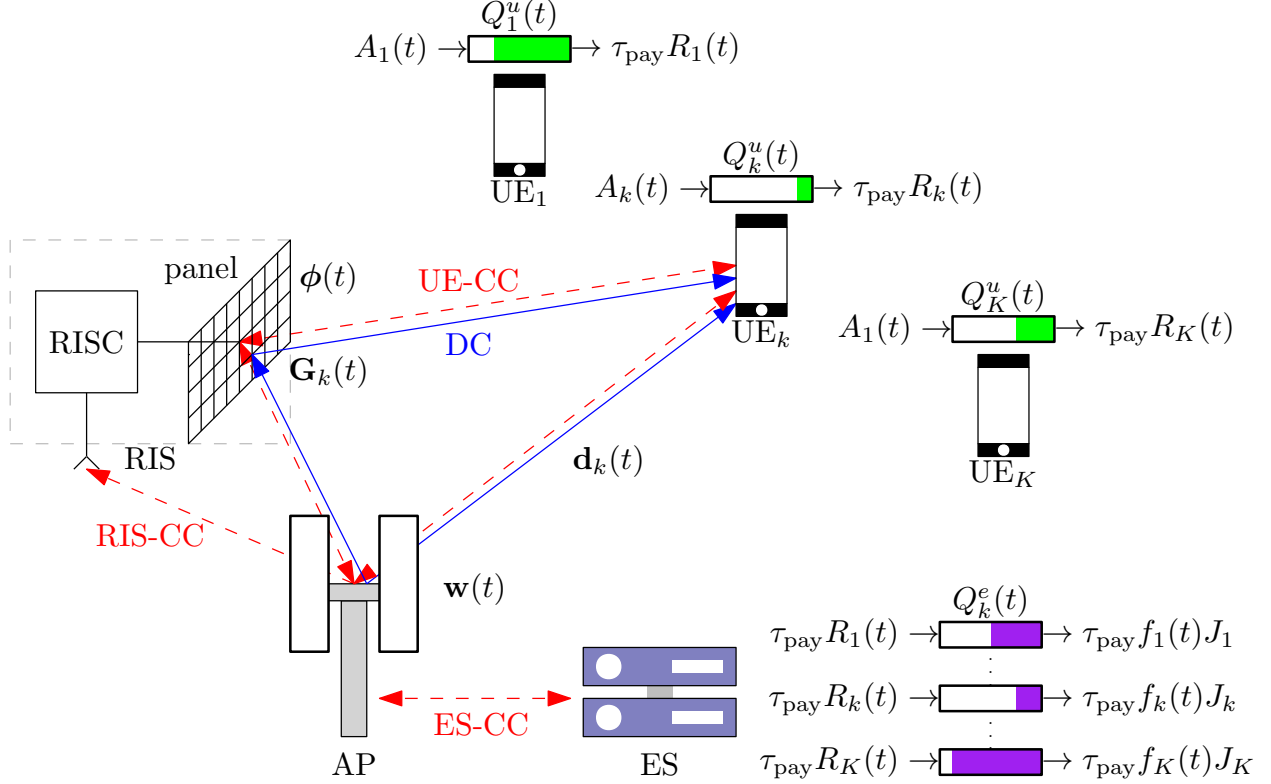


Figure 1: RIS-aided MEC system of interest: K single-antenna UEs offload their data to an ES, connected to a multi-antenna AP aided by a RIS, by transmitting a portion of their local queues $Q_k^u(t)$ in each slot t . The ES stores the data in remote queues $Q_k^e(t)$ and performs computation over them using CPU frequencies $f_k(t)$. To account for the control operations that dictate how the data is offloaded, a **data channel (DC)** and three **control channels (CCs)** are considered.

2.1 AP and RIS modeling

The AP enforces the synchronization of the system and controls the behavior of the RIS [13]. The AP is assumed to have analog beamforming capabilities, *i.e.*, it can load a beamforming vector $\mathbf{w}(t) \in \mathbb{C}^M$ with $\|\mathbf{w}(t)\| = 1$ to focus its transmission at the t -th slot. The set of possible available beamforming vectors forms the AP codebook denoted as \mathcal{C}_{ap} , modeled from accurate antenna patterns as in [15], such that $\mathbf{w}(t) \in \mathcal{C}_{\text{ap}}$.

The RIS device is made of a RIS controller (RIS) and a RIS panel [14]. The former receives control information from the AP and commands the changes of the electromagnetic properties of the latter. If activated, each element of the RIS panel can be tuned to impose a *phase-shift* variation on the impinging wave. At every slot t , the set of the states of all the elements forms the so-called *RIS configuration*, denoted as

$$\phi(t) = [\alpha_1(t)e^{j\phi_1(t)}, \dots, \alpha_N(t)e^{j\phi_N(t)}]^T \in \mathbb{C}^N, \quad (2)$$

where $\alpha_n(t) \in \{0, 1\}$ and $\phi_n(t) \in \{\frac{2i\pi}{2^b}\}_{i=0}^{2^b-1}$ represent the activation state and the (b -bit quantized) phase shift of the n -th RIS element, respectively. Without loss of generality, we assume the RIS needs τ_s seconds to load a new configuration due to its hardware characteristics. Moreover, we assume the RIS has a single receiver radio frequency (RF) chain to process the incoming control information from the AP. In particular, the RIS has a *wide-width beam control (ctl) configuration* $\phi_{\text{ctl}} \in \mathbb{C}^N$ that can boost the overall coverage of the AP in a certain area of interest where the UEs might be located. We assume the RIS always loads the control configuration when control signaling is exchanged between AP and UEs. The RIS is also equipped with a *CE codebook* \mathcal{C}_{ce} that contains $|\mathcal{C}_{\text{ce}}| = C_{\text{ce}}$ pre-defined configurations $\phi \in \mathcal{C}_{\text{ce}}$ used during the CE procedure, as defined in [16–18]. The CE procedure is presented in Section 3.

2.2 Channel modeling and control signaling

As shown in Fig. 1, we make use of four different channels: a data channel (DC) used by the UEs to transmit data to the AP and three different control channels (CCs) – UE-CC, RIS-CC, and ES-CC – used to exchange the control information of the UEs, the RIS, and the ES, respectively. In particular, the UE-CC represents the physical downlink

(DL) and uplink (UL) CC between the AP and the UEs (*e.g.*, PDCCH/PUCCH in 5G [19]), which is used for informing about scheduling, reporting channel quality, transmitting acknowledgment (ACK) signals, etc. The RIS-CC enables the AP to control the RIS behavior. The ES-CC coordinates the exchange of information over the backhaul link connecting the AP and the ES. In general, we use the *far-field assumption* when modeling the wireless channels, as in [13, 14, 20]. Moreover, we assume a *block-fading model*, *i.e.*, the wireless channels are static and frequency-flat within each slot. The choice of the slot duration τ can be thus related to the coherence time of the channel.

We assume that control signaling occurs through the transmission of *control packets* over the UE-CC and RIS-CC. A control packet has a duration of T seconds, defined as the system's minimum transmission time interval (TTI).

2.2.1 Data Channels (DCs)

Due to FDM, the k -th UE transmits data to the AP through its own DC, which is a UL channel operating with bandwidth B_k . The DC channel is denoted as $\mathbf{h}_k(t, \phi(t)) \in \mathbb{C}^M$ being a function of the slot t and the corresponding RIS configuration loaded. It can be written as

$$\mathbf{h}_k(t, \phi(t)) = \mathbf{d}_k(t) + \mathbf{G}_k(t)\phi(t), \quad (3)$$

where $\mathbf{d}_k(t) \in \mathbb{C}^M$ and $\mathbf{G}_k(t) \in \mathbb{C}^{M \times N}$ represent the direct UE-AP and the equivalent reflected UE-RIS-AP channel coefficients, respectively.

2.2.2 ES Control Channel (ES-CC)

The ES-CC is considered to be an out-of-band CC (CC), *i.e.*, the resources used for this channel are orthogonal w.r.t. the ones used for the DC, resulting in an instantaneous and error-free channel. This is because a system designer can easily make this CC as reliable as possible due to the high available pool of resources. Moreover, the ES and AP are most likely co-located and cable-connected in our scenario.

2.2.3 UE Control Channel (UE-CC)

The UE-CC of the k -th UE works over both DL and UL directions and is an in-band CC (CC), *i.e.*, its operational frequency and bandwidth overlap with the resources used for the DC of the k -th UE. This is considered to let the control signaling sent by the AP be aided by the RIS using the ctl configuration. Moreover, we assume control signaling is performed by exchanging control packets transmitted to or from the UEs, whose packets are sent using bandwidth B_k .

2.2.4 RIS Control Channel (RIS-CC)

We assume that the AP controls the RIS over a wireless DL connection. We analyze the RIS-CC in the IB-CC condition that considers that the resources of this channel overlap with the ones of the DCs. Thus, control signaling for RIS control cannot co-occur with transmissions for/from UEs. It is assumed that control signaling on this CC is performed through control packets transmitted by the AP over bandwidth B .

2.3 Dynamic queuing modeling

Following [13], we consider a dynamic queuing system, where each UE has a *local communication queue* to buffer data to be transmitted/offloaded, while the ES has a *remote computation queue* to buffer data to be processed. We present the general update rules of these queues below.

Let $\tilde{R}_k(t)$ denote the *actual throughput* of the k -th UE at slot t , $k \in \mathcal{K}$. We denote as $Q_k^u(t)$ the local communication queue of the k -th UE, updated as follows

$$Q_k^u(t+1) = \max[0, Q_k^u(t) - \tau_{\text{pay}}\tilde{R}_k(t)] + A_k(t), \quad (4)$$

where $A_k(t)$ [bits] is the realization of the data arrival process at slot t .

Let f_{max} be the total CPU frequency of the ES. Let Q_k^e denote the remote computation queue for the k -th UE at the ES. We assume that the ES allocates computational resource $f_k(t)$ to process the task offloaded by the k -th UE at slot t , such that $\sum_{k \in \mathcal{K}} f_k(t) = f_{\text{max}}$. Thus, the remote computation queue for the k -th UE at the ES evolves as

$$Q_k^e(t+1) = \max[0, Q_k^e(t) - \tau_{\text{pay}}f_k(t)J_k] + \min\left(Q_k^u(t), \tau_{\text{pay}}\tilde{R}_k(t)\right), \quad (5)$$

where J_k [bit/Hz/s] is an efficiency parameter that depends on the application offloaded by the k -th UE.

The *total queue* for the k -th UE can be described as

$$Q_k(t) = Q_k^u(t) + Q_k^e(t). \quad (6)$$

The *average offloading latency* perceived by the k -th UE is

$$L_k(t) = Q_k(t)/\bar{A}_k, \quad (7)$$

where $\bar{A}_k = \mathbb{E}_{\sim t}[A_k(t)]/\tau$ is the average arrival rate [kbps].

2.4 Energy consumption modeling

The total energy consumption in the system is modeled as a weighted sum of the energy consumed by the ES, AP, RIS, and the UEs at each slot, denoted as $E_e(t)$, $E_a(t)$, $E_r(t)$, and $E_k(t)$, respectively. Based on [13], we have the following total energy consumption at slot t

$$E_\sigma^{\text{tot}}(t) = \sigma \sum_{k \in \mathcal{K}} E_k(t) + (1 - \sigma)(E_e(t) + E_a(t) + E_r(t)), \quad (8)$$

where $\sigma \in [0, 1]$ is a weighting parameter striking a trade-off between UE and network consumption; choosing $\sigma = 1$ leads to a pure user-centric strategy; whereas, $\sigma = 0$ induces a pure network-centric strategy. Below, we model each one of the energy terms, where, different from [13], we introduce the energy consumption related to control operations.

The energy consumption at the ES depends on the computation tasks over offloaded data and control operations. Modeling the energy spent for computation using a complementary metal-oxide semiconductor (CMOS)-based CPU [21], we obtain that the ES consumes

$$E_e(t) = \tau_{\text{pay}} \gamma_c f_{\text{max}}^3 + E_e^{\text{ctl}}(t), \quad (9)$$

where γ_c is the effective switching capacitance of the ES processor, and E_e^{ctl} is the ES energy consumption related to control.

The energy spent by the k -th UE depends on the data transmission and control operations and is given by

$$E_k(t) = \tau_{\text{pay}} P_k(t) + E_k^{\text{ctl}}(t), \quad (10)$$

where $P_k(t)$ is the power spent by the k -th UE for data transmission, and $E_k^{\text{ctl}}(t)$ is the k -th UE energy consumption related to control for $k \in \mathcal{K}$.

Since we consider UL data transmissions, the AP spends energy only for control operations, given by

$$E_a(t) = E_a^{\text{ctl}}(t). \quad (11)$$

The RIS energy consumption depends on the power dissipated by its active elements and control operations, which can be modeled as

$$E_r(t) = \tau_{\text{pay}} P_r(b) \sum_{n \in \mathcal{N}} \alpha_n(t) + E_r^{\text{ctl}}(t), \quad (12)$$

where $P_r(b)$ is the power dissipated by each of the N b -bit resolution elements of the RIS, $\alpha_n(t) \in \{0, 1\}$ is the element activation state (see eq. (2)), and $E_r^{\text{ctl}}(t)$ is the RIS energy consumption related to control.

In Section 4, we will specify the energy consumed due to control operations for all the communication nodes.

3 Offloading Protocol with Control Operations

In this section, we present the protocol dictating how the computation offloading service occurs in a RIS-aided MEC system when considering its control aspects. Before the beginning of the offloading procedure, we assume that the UEs connect to the network through an *access phase*. During this phase, the AP grants access to the UEs by allocating the bandwidths B_k 's for the DCs according to frequency multiplexing. Moreover, the AP broadcasts essential protocol details, including the slot duration τ and other pertinent information, to all the UEs. The proper design of this phase is beyond the scope of this paper (*e.g.*, see [20]).

Fig. 2 shows the timing diagram of the protocol within the t -th slot. In Section 2, we have defined that each slot of duration τ is divided into control τ_{ctl} and payload τ_{pay} times (see eq. (1)). Following the framework introduced in [14], we further divide the control overhead into three different phases related to two different types of control operations: *signaling* and *algorithmic*. Thus, each slot consists of two signaling phases, *initialization* and *setup*, in which control

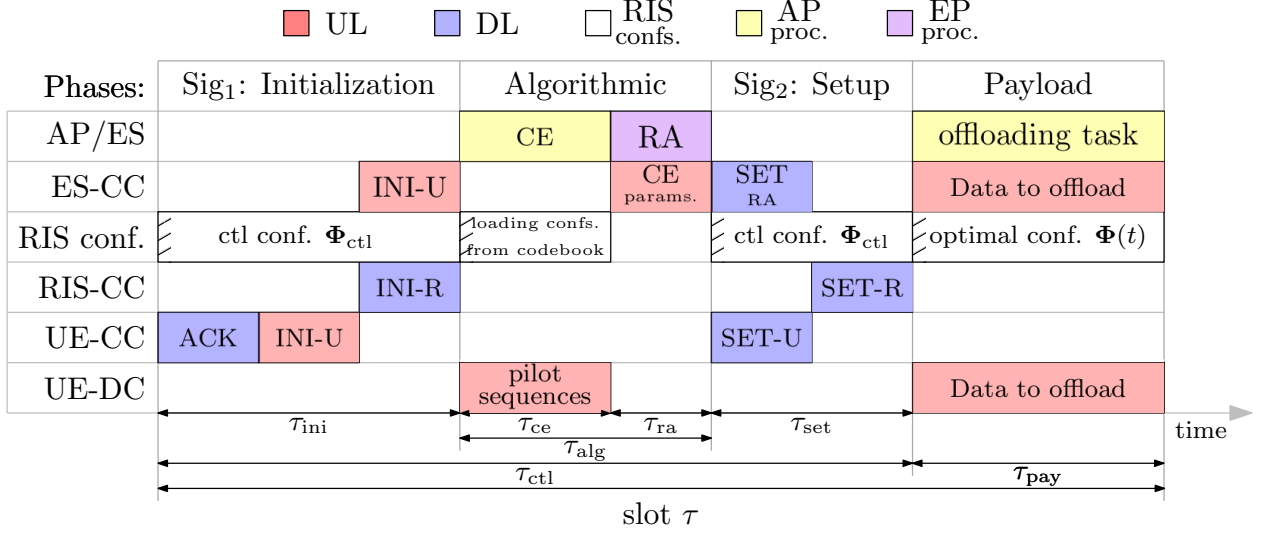


Figure 2: A timing diagram illustrating the offloading protocol execution at time slot t . The slot is divided into four phases: a) Signaling – initialization, b) algorithmic, c) Signaling – setup, and d) payload. The first three phases occur within the control time τ_{ctl} while the latter occurs over the payload time τ_{pay} . Control signaling is implemented through the introduction of four control packets: INI-U, with initial information sent by the UE to the AP; INI-R, with initial information sent by the AP to the RIS; SET-U, with optimized RA parameters sent by the AP to the UE; and SET-R, with an optimal configuration, $\phi(t)$, sent by the AP to the RIS.

information needed to initialize the network and set the optimized parameters of the offloading service are exchanged between nodes, respectively; an *algorithmic* phase comprising the processing times of the CE and RA operations, which are needed to optimize the offloading service; and a *payload* phase in which data transmission and offloading take place. The duration of these four phases is denoted as τ_{ini} , τ_{alg} , τ_{set} , and τ_{pay} , respectively. By definition, we have that $\tau_{\text{ctl}} = \tau_{\text{ini}} + \tau_{\text{alg}} + \tau_{\text{set}}$, and we can rewrite eq. (1) as

$$\tau = \tau_{\text{ctl}} + \tau_{\text{pay}} = \tau_{\text{ini}} + \tau_{\text{alg}} + \tau_{\text{set}} + \tau_{\text{pay}}. \quad (13)$$

Next, we detail each phase within the t -th slot.

3.1 Signaling: Initialization phase

During this phase, the RIS loads the ctl configuration, ϕ_{ctl} (see Section 2.1). The AP starts by carrying out an ACK procedure that informs the UEs about the correct decoding of received data on the previous slot by broadcasting ACK/NACK packets, one packet per UE. The UEs prepare the data to offload accordingly, *i.e.*, if the k -th UE received a NACK, it re-inserts the data unsuccessfully transmitted as the oldest data in its queue $Q_k^u(t)$. Afterward, the UEs inform the AP on the state of their communication queues $Q_k^u(t)$, where each UE sends a control packet called INI-U through the UE-CC. This information is then propagated to the ES through the ES-CC because the ES needs it as input to perform the RA. Meanwhile, the AP informs the RIS to be prepared to start the CE operation by sending a control packet called INI-R over the RIS-CC.

3.2 Algorithmic phase

The algorithm phase consists in the CE and RA procedures, having duration τ_{ce} and τ_{ra} , respectively, with $\tau_{\text{alg}} = \tau_{\text{ce}} + \tau_{\text{ra}}$.

We start by describing the CE procedure. The CE operation takes place through the transmission of pilot sequences by the UEs to the AP. Then, the AP uses the received signals to estimate the CSI comprised of direct channels $\mathbf{d}_k(t)$ and the equivalent reflected channels $\mathbf{G}_k(t)$, $\forall k \in \mathcal{K}$ by using one of the possible CE methods for RIS-aided systems, *e.g.*, [16–18]. In general, these methods estimate the channels using a two-step process: i) the UEs transmit pilot sequences while the RIS is turned off, *i.e.*, $\phi = \mathbf{0}_N$; then, the AP estimates the direct channel; ii) the UEs transmit replicas of the pilot sequences while the RIS sweeps through a *CE codebook* \mathcal{C}_{ce} containing RIS configurations $\phi \in \mathcal{C}_{\text{ce}}$ – a configuration is loaded per each pilot replica²; then, the AP can subtract the direct channel from the received

²Note that \mathcal{C}_{ce} need to be shared among the AP and the RIS, while the UEs know its cardinality $|\mathcal{C}_{\text{ce}}| = C_{\text{ce}}$ to transmit an adequate number of pilot sequences; the information about \mathcal{C}_{ce} and C_{ce} can be exchanged during the access phase.

signals and apply any classical estimation technique to estimate the reflected channels, taking care of removing the influences of the used configurations in \mathcal{C}_{ce} [17, 18]. The overall estimated CSI for the k -th UE is denoted as $\hat{\mathbf{h}}(t, \phi) = \hat{\mathbf{d}}_k(t) + \hat{\mathbf{G}}_k(t)\phi$, for any ϕ . The AP shares the CSI knowledge obtained with the ES.

We now describe the RA procedure. The ES can perform a RA procedure based on the estimated CSI, on the knowledge of the UEs local communication queues given by the transmission of INI-U packets, and on its remote computation queues. We adopt the RA procedure introduced in [13]. This procedure minimizes the total energy consumption while constraining the perceived average offloading latency under a threshold, \bar{L} . This is done by leveraging Lyapunov stochastic optimization in a greedy manner that optimizes the following parameters: 1) the AP beamforming vector $\mathbf{w}(t)$, 2) the UEs power coefficients denoted as $P_k(t)$, 3) the ES offloading computation resources $f_k(t)$, $\forall k \in \mathcal{K}$, and 4) the RIS configuration $\phi(t)$ (see [13] for further details on the optimization).

3.3 Signaling: Setup phase

During this phase, the RIS again loads the ctrl configuration, ϕ_{ctrl} (see Section 2.1). This phase aims to send the parameters optimized by the RA, carried out during the algorithmic phase by the ES, to the UEs and the RIS. First, the ES sends the RA parameters towards the AP through the ES-CC. Then, the AP sends control packets called SET-U to each UE containing its power coefficient $P_k(t)$ and its nominal throughput $R_k(t)$ over the UE-CC. Similarly, the AP sends a control packet called SET-R to the RIS containing the configuration $\phi(t)$ over the RIS-CC.

3.4 Payload phase

In this phase, every UE offloads its data by transmitting with its power coefficient $P_k(t)$ and its nominal throughput $R_k(t)$ while the RIS loads the configuration $\phi(t)$ and the AP employs the beamforming vector $\mathbf{w}(t)$. Accordingly, it is expected that the k -th UE transmits with power $P_k(t)$ and *nominal throughput* $R_k(t)$ given by

$$R_k(t) = B_k \log \left(1 + \frac{P_k(t)}{N_0 B_k} |\mathbf{w}(t)^H \hat{\mathbf{h}}_k(t, \phi(t))|^2 \right), \quad (14)$$

where N_0 [W/Hz] is the noise spectral density. In the ideal case of perfect CSI with error-free CCs, the UE can reliably transmit at its channel capacity, given by³

$$C_k(t) = B_k \log_2 \left(1 + \frac{P_k(t)}{N_0 B_k} |\mathbf{w}(t)^H \mathbf{h}_k(t, \phi(t))|^2 \right). \quad (15)$$

In this case, the actual throughput in (4) and the nominal throughput in (14) are the same as $\tilde{R}_k(t) = R_k(t) = C_k(t)$. However, we are interested in studying cases in which the control operations are not error-free. Specifically, errors in the CE or the control signaling may lead to a nominal throughput higher than the channel capacity, resulting in the loss of the payload data. Hence, the actual throughput used to empty the UE queues in (4) and (5) evaluates to

$$\tilde{R}_k(t) = \begin{cases} 0, & \text{if } R_k(t) > C_k(t), \\ R_k(t), & \text{if } R_k(t) \leq C_k(t). \end{cases} \quad (16)$$

We analyze the impact of the control operations in the next section.

4 Impact of Control Operations

In this section, we analyze the impact of control operations on the perceived offloading delay and the total energy consumption of the system. We first evaluate the overhead and the energy consumption introduced by the control operations; then, we describe how losing the control packets affects the decisions of the nodes.

4.1 Overhead evaluation

The control overhead τ_{ctrl} accounts for the time reserved for all control operations, which depends on the number of control packets sent during the initialization and setup phases and the duration of the CE and RA procedures during the algorithmic phase. Next, we characterize the control overhead of eq. (13).

³We are assuming to work on the Shannon limit for simplicity of presentation. A real system should account for the loss provided by the modulation and coding scheme (MCS) used.

Signaling: Initialization phase The control overhead due to the initialization phase consists of i) the simultaneous transmission of K one-bit messages for the ACK procedure, ii) the simultaneous transmission of K INI-U control packets, and iii) the transmission of a single INI-R control packet. Moreover, we consider a guard period of τ_s seconds to load the ctl configuration. Thus, the initialization overhead is

$$\tau_{\text{ini}} = \tau_s + 3T. \quad (17)$$

Algorithmic phase Due to FDM, the CE of each UE is performed simultaneously. In each bandwidth B_k , the k -th UE transmits a pilot sequence composed of N_p TTIs for the direct path estimation, and the same sequence is repeated for each RIS configuration in the CE codebook C_{ce} for the reflected path estimation. The CE overhead results in

$$\tau_{\text{ce}} = (\tau_s + N_p T)(C_{\text{ce}} + 1), \quad (18)$$

where τ_s is the switching time between each configuration and C_{ce} is the number of CE configurations.

The RA overhead τ_{ra} is determined by the number of computational cycles required in RA task n_{ra} and by the CPU cycles f_{ra} [cycle/s] employed for computation, obtaining:

$$\tau_{\text{ra}} = \frac{n_{\text{ra}}}{f_{\text{ra}}}, \quad (19)$$

where $f_{\text{ra}} \leq f_{\text{max}}$. To evaluate n_{ra} , we only consider the cost of jointly optimizing the RIS configuration and AP beamforming vector and ignore the power coefficient computation, the latter needed regardless of the presence of the RIS. Following [13, Algorithm 1], the optimal $\phi(t)$ and $\mathbf{w}(t)$ are obtained employing a greedy approach: keeping fixed an AP beamforming vector $\mathbf{w}(t) \in \mathcal{C}_{\text{ap}}$, we select the phase-shift that minimizes the objective function in [13, eq. (26)] for a group of $N_g < N$ elements, keeping fixed the phase-shifts of the other elements $N - N_g$. Considering that each element can be inactive or active with 2^b different phase-shift values, the number of possible choices is $2^b + 1$. Note that the N_g elements grouped will load the same phase-shift. This procedure is repeated $\forall \mathbf{w}(t) \in \mathcal{C}_{\text{ap}}$ to find the pair $(\mathbf{w}(t), \phi(t))$ that greedily minimizes the objective function. Accordingly, the number of computational cycles yields in

$$n_{\text{ra}} = C_{\text{ap}}(2^b + 1) \frac{N}{N_g} \mu, \quad (20)$$

where $\mu = 2[K(3N/N_g + M + 4) + 3]$ is the number of multiplications needed to evaluate the objective function for every pair $(\mathbf{w}(t), \phi(t))$ [13, Algorithm 1]⁴. Clearly, the performance boost provided by the RIS can be maximized by applying this procedure for each element, *i.e.*, by setting $N_g = 1$, at the cost of increasing τ_{ra} .

Signaling – setup phase The control overhead due to the setup phase consists of i) the simultaneous transmission of K SET-U control packets and ii) the transmission of a single SET-R control packet. Again, we consider the guard period of τ_s seconds to load the ctl configuration. Thus, the setup overhead is:

$$\tau_{\text{set}} = 2\tau_s + 2T. \quad (21)$$

4.2 Energy consumption due to control operations

We now characterize $E_e^{\text{ctl}}(t)$, $E_k^{\text{ctl}}(t)$, $E_a^{\text{ctl}}(t)$ and $E_r^{\text{ctl}}(t)$ introduced in Section 2.4. For the ES, the energy spent during the control portion of the slot is the energy used to perform the RA, modeled in the same way as the offloading task, obtaining

$$E_e^{\text{ctl}}(t) = \gamma_c f_{\text{ra}}^3 \tau_{\text{ra}}. \quad (22)$$

During control signaling, each k -th UE sends only a single INI-U packet; for CE, it sends $C_{\text{ce}} + 1$ pilot sequences of length N_p TTIs. Hence, the energy consumption during control is

$$E_k^{\text{ctl}}(t) = P_k^{\text{ctl}}(t)T(1 + N_p(C_{\text{ce}} + 1)), \quad (23)$$

where $P_k^{\text{ctl}}(t)$ is the power used for control signaling. The AP consumes power to send control packets. It sends the ACK and SET-U packets to all the K UEs, while the INI-R and SET-R packets to a single receiver; hence, it consumes

$$E_a^{\text{ctl}}(t) = 2P_a^{\text{ctl}}(t)T(K + 1), \quad (24)$$

where $P_a^{\text{ctl}}(t)$ is the AP power used for control signaling. Finally, we assume that all the RIS elements are active when loading ϕ_{ctl} and during the CE of the reflected path, yielding

$$E_r^{\text{ctl}}(t) = (\tau_{\text{ini}} + \tau_{\text{set}} + C_{\text{ce}}N_pT)NP_r(b). \quad (25)$$

⁴We used the multiplication as the dominant operations for simplicity.

4.3 The effect of control errors

The performance of the overall network is tied with the actual throughput $\tilde{R}_k(t)$, dependent on the nominal throughput $R_k(t)$ and the possible errors in the CE and in the control signaling that can occur when decoding the control packets.

Errors in CE The following proposition characterizes the estimation error during CE.

Proposition 1. *Assuming least squares (LS) estimation applied on pilot replicas of N_p symbols length and uncorrelated Rayleigh channels, the CSI at the AP after the CE is*

$$\begin{aligned}\hat{\mathbf{d}}_k(t) &= \mathbf{d}_k(t) + \mathbf{n}_k(t) \sim \mathcal{CN}(\mathbf{0}_M, \lambda_k \mathbf{I}_M), \\ \hat{\mathbf{G}}_k(t) &= \mathbf{G}_k + \mathbf{N}_k(t) \sim \mathcal{CN}(\mathbf{0}_{MN}, \gamma_k \mathbf{I}_{MN}),\end{aligned}\quad (26)$$

having variances

$$\lambda_k = \frac{N_0 B_k}{N_p P_k^{\text{ctl}}(t)}, \quad \gamma_k = \frac{2N_0 B_k}{N_p P_k^{\text{ctl}}(t)} \frac{N}{C_{\text{ce}}^2}. \quad (27)$$

Proof. The expression of the $\hat{\mathbf{d}}_k(t)$ is derived by correlating the received signal with the transmitted pilot when $\phi(t) = \mathbf{0}_N$; then $\hat{\mathbf{G}}_k(t)$ is obtained by correlating the received signal with the pilot, subtracting $\hat{\mathbf{d}}_k$, and post-multiply it by the configurations in \mathcal{C}_{ce} [17]. \square

Errors in control signaling If correct control occurs, *i.e.*, no control packet is lost or erroneously decoded, the transmission power $P_k(t)$ and the nominal throughput $R_k(t)$ in (14) are correctly set by the UE. In the following, we detail the effect on the decision made by the nodes caused by losing each of the control packets⁵ – INI-U, INI-R, SET-U, SET-R.

If the k -th UE's INI-U packet is lost, the information on the UE local queue is not provided to the ES; then, the latter can infer from the received data that the UE communication queue was emptied by $\tau_{\text{pay}} \tilde{R}_k(t)$ bits. Since the ES is still unaware of the amount of new data $A_k(t)$ arrived at the UE, its queue is updated following

$$\hat{Q}_k^u(t+1) = \max[0, Q_k^u(t) - \tau_{\text{pay}} \tilde{R}_k(t)]. \quad (28)$$

The RA process will use this input to optimize the power coefficient and the nominal throughput, impacting the offloading latency.

If the INI-R packet is not received, the RIS is unaware of the need for switching configurations for the CE process. Then, the whole CE procedure occurs while the RIS loads the control configuration ϕ_{ctrl} . For the sake of simplicity, we assume that no CSI can be obtained in this case, and the nominal throughput of all UEs result in $R_k(t) = 0$, $\forall k \in \mathcal{K}$.

If the k -th UE's SET-U packet is lost, then the k -th UE is not informed by the power coefficient $P_k(t)$ and the nominal throughput $R_k(t)$ in (14) for the payload transmission. Hence, the best the UE can do is to transmit with the power and the throughput of the previous slot, hoping the data stream can be decoded at the AP. We have

$$P_k(t) = P_k(t-1) \text{ and } R_k(t) = R_k(t-1). \quad (29)$$

If the SET-R packet is not received, the RIS is not informed of $\phi(t)$ and can only resort to loading the optimal configuration of the previous slot. This affects the channel capacity of the system, being now, $\forall k \in \mathcal{K}$,

$$C_k(t) = B_k \log_2 \left(1 + \frac{P_k(t)}{N_0 B_k} |\mathbf{w}(t)^H \mathbf{h}_k(t, \phi(t-1))|^2 \right). \quad (30)$$

Note that the reliability of the control packets depends on their informative content, the time reserved for the transmission, and the bandwidth of the CCs. In this paper, the impact of reliability will be analyzed numerically.

5 Numerical Results

In this section, we numerically evaluate the impact of control operations in the QoS of the computation offloading service in RIS-aided MEC systems. The presented results are obtained simulating a scenario similar to Fig. 1: the

⁵The ACK packet is not analyzed because it is needed regardless of the presence of a RIS in the system. Hence, the ACK packet is always reliable, an assumption justified by its limited informative content.

Table 1: Simulation parameters.

Scenario radius	r	100 m
AP position	\mathbf{x}_a	$50\sqrt{2}[1, 1, 0]^T$ m
RIS elements	N	64
AP antennas	M	8
No. of UEs	K	4
No. of slots	N_t	100
Overall bandwidth	B	500 MHz
UE/AP ctl power	$P_k^{\text{ctl}}(t), P_a^{\text{ctl}}(t)$	20, 24 dBm
UE/AP noise density	N_0	-170 dBm/Hz
Gain at reference distance	σ_0^2	-38 dB m ²
Max. and RA CPU freq.	$f_{\text{max}}, f_{\text{ra}}$	4.5, 0.5 GHz
Avg. arrival rate	\bar{A}_k	[50, 100, 200] kbps
Avg. latency constraint	\bar{L}	300 ms
Energy weighting parameter	σ	0.5
Codebooks cardinality	$C_{\text{ap}}, C_{\text{ce}}$	25, N
Slot, TTI, RIS guard time	τ, T, τ_s	60 : 300, 1/14, 0 ms
Pilot sequence length	N_p	1
Group of RIS elements	N_g	2

RIS is positioned at the center of a semi-circle of radius r , while the AP's position is $\mathbf{x}_a \in \mathbb{R}^3$; for every setup under test, the K UEs have random positions $\mathbf{x}_k \in \mathbb{R}^3$ within the semi-circle, and N_t different slots are simulated. The presented results are averaged for the different setups if not specified differently. The channels are generated following Rayleigh fading, *i.e.*, $\mathbf{d}_k(t) \sim \mathcal{CN}(\mathbf{0}_M, \sigma_0^2 \|\mathbf{x}_a - \mathbf{x}_k\|^{-3} \mathbf{I}_M)$, and $[\mathbf{G}_k(t)]_m = (\mathbf{r}_k(t) \circ \mathbf{g}_m(t))^T, \forall m \in \mathcal{M}$, with $\mathbf{g}_m(t) \sim \mathcal{CN}(\mathbf{0}_N, \sigma_0^2 \|\mathbf{x}_a\|^{-2} \mathbf{I}_N)$ being the RIS-AP channel, and $\mathbf{r}_k(t) \sim \mathcal{CN}(\mathbf{0}_N, \sigma_0^2 \|\mathbf{x}_k\|^{-2} \mathbf{I}_N)$ the UE-RIS one. The other relevant parameters are listed in Table 1 [13, 14]⁶. With the parameters under test, the overall control overhead results in $\tau_{\text{ctl}} = 50.2$ ms, composed by $\tau_{\text{ini}} + \tau_{\text{set}} = 3.6$ ms, $\tau_{\text{ce}} = 46.4$ ms, and $\tau_{\text{ra}} \approx 0.17$ ms with $\tau_{\text{alg}} = \tau_{\text{ce}} + \tau_{\text{ra}}$. This demonstrates that the CE impact on the overhead is dominant, constraining the whole system to work with time granularity that can hardly be met in practical scenarios. Hence, further research targeting the reduction of the CE burden is needed to integrate the RIS in real systems.

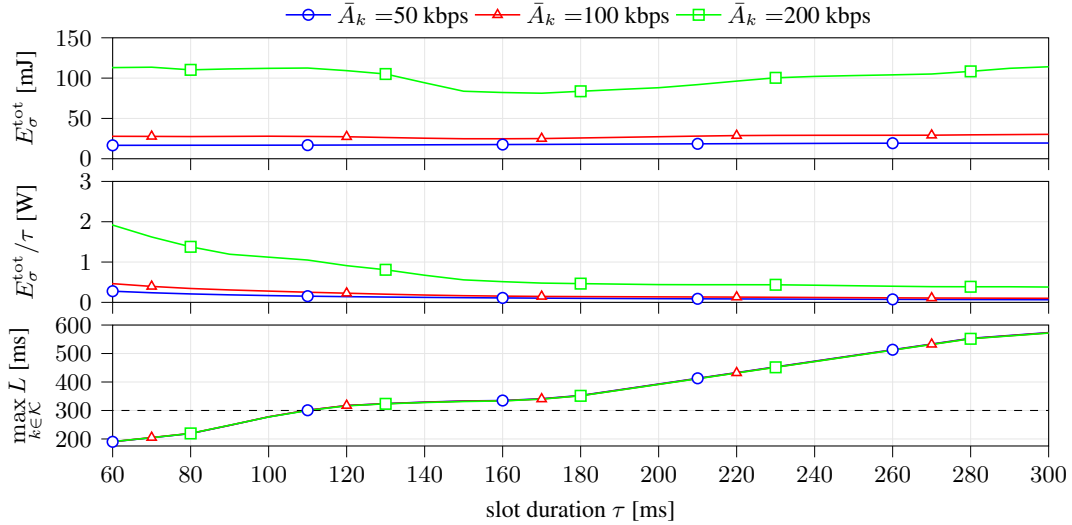


Figure 3: System performance vs. slot duration (error-free).

Fig. 3 shows the average energy consumption, the average power spent per slot, and the maximum offloading latency as a function of the slot duration τ , considering an error-free environment, *i.e.*, with perfect CSI knowledge, and perfect control signaling. The parameters simulate a scenario where the coherence time is 300 ms, and the slot duration can be set to strike an energy-latency trade-off. Note that the control overhead is fixed, resulting in an increased payload time τ_{pay} when τ increases, following (13). While the selection of the slot duration slightly influences the average energy consumption, the power spent per slot reduces with increasing τ due to the possibility of decreasing the nominal

⁶See <https://github.com/victorcroisfelt/mec-with-ris-control> for the code.

throughput and the ES CPU frequency while transmitting and processing the same amount of bits. On the other hand, increasing τ directly increases the offloading latency experienced, risking violating the latency constraint. Moreover, an eventual increase of \bar{A}_k is absorbed by higher energy consumption without impacting the latency performance. Hence, the optimal working point is given by the highest slot time able to support the latency constraint, which is around $\tau = 100$ ms for our scenario.

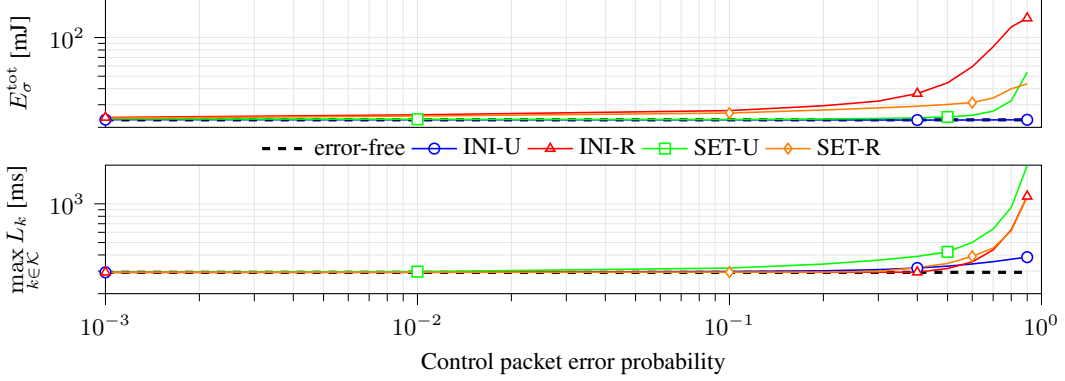


Figure 4: System performance vs. control packet error probability ($\tau = 100$ ms, $\bar{A}_k = 50$ kbps).

Fig. 4 shows the system performance as a function of the control packet error probability, assuming that each curve simulates that only one kind of control packet can be lost. Losing INI-U packets influences the performance the least, showing that the system can generally recover the arrival rate information in subsequent slots. Losing INI-R packets strongly affects energy consumption while moderately influencing latency because the system tends to spend more energy to offload more data after an unsuccessful CE. Losing SET-U packets strongly affects the latency performance due to the use of the inaccurate value of $P_k(t)$ and $R_k(t)$, while an inaccurate $\phi(t)$ is less harmful (see SET-R).

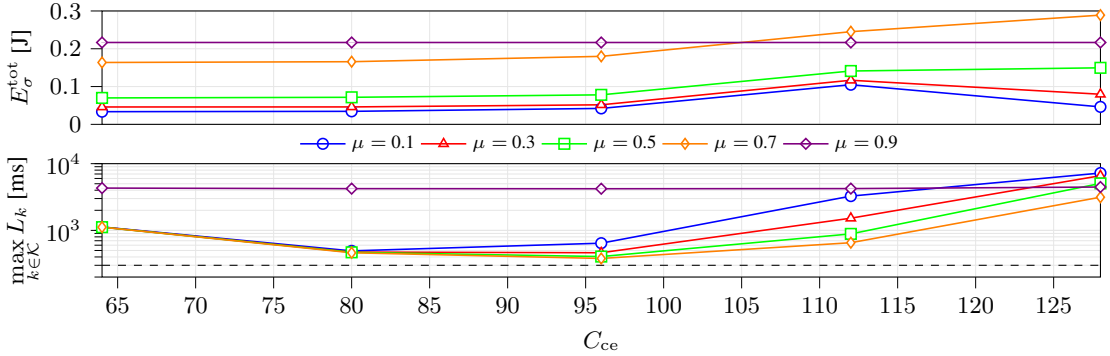


Figure 5: System performance vs. the number of CE configurations ($\tau = 100$ ms, $\bar{A}_k = 100$ kbps).

Finally, Fig. 5 shows the performance when accounting for the CE errors as a function of the number of CE configurations, C_{ce} . In this case, to reduce the probability that $R_k(t) > C_k(t)$, the nominal throughput is multiplied by a discount factor $\mu \leq 1$. Under these conditions, the system is not able to provide the desired QoS regardless of the value of μ and C_{ce} , demonstrating the need to account for the control errors during the RA, eventually optimizing the value of μ^7 . When a low value of μ is used, $\mu R_k(t) \leq C_k(t)$ is probable, but the resulting throughput is insufficient to follow the arrival rate process. When μ is close to 1, it is likely that $\mu R_k(t) > C_k(t)$, resulting in a failed offload operation on slot t . Also, the results confirm the expected: a small codebook leads to worse CE performance but higher payload time while increasing C_{ce} leads to a lower payload time but better CE performance.

6 Conclusions

In this paper, we have analyzed the control aspects related to MEC aided by RIS. Our investigation has highlighted the necessity of considering the various control operations when designing optimization algorithms for these services.

⁷Remark that the CE of the direct channels is influenced by N_p only, which should also be set to a proper value in a real system.

In particular, the results demonstrate that the CE procedure has the dominant impact on the UEs QoS, generating the highest overhead and greatly influencing the RA due to the CSI errors. Future works will capitalize on these findings, investigating possible robust RA strategies along with the control operations.

References

- [1] S. Ahmadi, *5G NR: Architecture, Technology, Implementation, and Operation of 3GPP New Radio Standards*. Elsevier Science, 2019.
- [2] E. Calvanese Strinati *et al.*, “6G: The next frontier: From holographic messaging to artificial intelligence using subterahertz and visible light communication,” *IEEE Vehicular Technology Magazine*, vol. 14, no. 3, pp. 42–50, Sep. 2019.
- [3] S. Barbarossa *et al.*, “Communicating while computing: Distributed mobile cloud computing over 5G heterogeneous networks,” *IEEE Signal Proc. Mag.*, vol. 31, no. 6, pp. 45–55, 2014.
- [4] C. Liu *et al.*, “Dynamic Task Offloading and Resource Allocation for Ultra-Reliable Low-Latency Edge Computing,” *IEEE Trans. on Commun.*, vol. 67, no. 6, pp. 4132–4150, 2019.
- [5] M. Merluzzi *et al.*, “Dynamic Computation Offloading in Multi-Access Edge Computing via Ultra-Reliable and Low-Latency Commun.” *IEEE Trans. on Signal and Information Process. over Networks*, pp. 1–1, 2020.
- [6] D. Han *et al.*, “Joint channel and queue aware scheduling for latency sensitive mobile edge computing with power constraints,” *IEEE Trans. on Wireless Commun.*, vol. 19, no. 6, pp. 3938–3951, 2020.
- [7] M. Merluzzi *et al.*, “Discontinuous computation offloading for energy-efficient mobile edge computing,” *IEEE Trans. on Green Commun. and Networking*, 2021.
- [8] E. Björnson *et al.*, “Reconfigurable intelligent surfaces: A signal process. perspective with wireless applications,” *IEEE Signal Process. Mag.*, vol. 39, no. 2, pp. 135–158, 2022.
- [9] T. Bai *et al.*, “Reconfigurable intelligent surface aided mobile edge computing,” *IEEE Wireless Commun.*, vol. 28, no. 6, pp. 80–86, 2021.
- [10] Z. Chu *et al.*, “Intelligent reflecting surface assisted mobile edge computing for internet of things,” *IEEE Wireless Commun. Letters*, 2020.
- [11] S. Huang *et al.*, “Reconfigurable intelligent surface assisted mobile edge computing with heterogeneous learning tasks,” *IEEE Trans. on Cognitive Commun. and Netw.*, 2021.
- [12] X. Hu *et al.*, “Reconfigurable intelligent surface aided mobile edge computing: From optimization-based to location-only learning-based solutions,” *IEEE Trans. on Commun.*, 2021.
- [13] P. D. Lorenzo *et al.*, “Dynamic edge computing empowered by reconfigurable intelligent surfaces,” *EURASIP Journal on Wireless Commun. and Networking*, vol. 2022, no. 1, Dec. 2022.
- [14] F. Saggese *et al.*, “On the impact of control signaling in RIS-empowered wireless communications,” 2023.
- [15] A. Clemente *et al.*, “Focal distance reduction of transmit-array antennas using multiple feeds,” *IEEE Antennas and Wireless Propagation Letters*, vol. 11, pp. 1311–1314, 2012.
- [16] A. L. Swindlehurst *et al.*, “Channel estimation with reconfigurable intelligent surfaces– A general framework,” *Proc. IEEE*, vol. 10, no. 9, pp. 1312–1338, Sep. 2022.
- [17] Z. Wang *et al.*, “Channel estimation for intelligent reflecting surface assisted multiuser commun.: Framework, algorithms, and analysis,” *IEEE Trans. Wireless Commun.*, vol. 19, no. 10, pp. 6607–6620, 2020.
- [18] L. Mo *et al.*, “Direct tensor-based estimation of broadband mmWave channels with RIS,” *IEEE Commun. Lett.*, vol. 27, no. 7, pp. 1849–1853, Jul. 2023.
- [19] 3GPP, “NR; Physical layer procedures for data,” 3rd Generation Partnership Project (3GPP), Technical specification (TS) 38.214, 10 2022, version 15.0.0.
- [20] V. Croisfelt *et al.*, “Random access protocol with channel oracle enabled by a reconfigurable intelligent surface,” *IEEE Trans. on Wireless Commun.*, pp. 1–1, 2023.
- [21] T. D. Burd *et al.*, “Processor design for portable systems,” *Journal of VLSI signal Process. systems for signal, image and video technology*, vol. 13, no. 2-3, pp. 203–221, 1996.